ORIGINAL PAPER

Analysis of high-resolution simulations for the Black Forest region from a point of view of tourism climatology – a comparison between two regional climate models (REMO and CLM)

Christina Endler · Andreas Matzarakis

Abstract An analysis of climate simulations from a point of view of tourism climatology based on two regional climate models, namely REMO and CLM, was performed for a regional domain in the southwest of Germany, the Black Forest region, for two time frames, 1971–2000 that represents the twentieth century climate and 2021–2050 that represents the future climate. In that context, the Intergovernmental Panel on Climate Change (IPCC) scenarios A1B and B1 are used. The analysis focuses on human-biometeorological and applied climatologic issues, especially for tourism purposes – that means parameters belonging to thermal (physiologically equivalent temperature, PET), physical (precipitation, snow, wind), and aesthetic (fog, cloud cover) facets of climate in tourism. In general, both models reveal similar trends, but differ in their extent. The trend of thermal comfort is contradicting: it tends to decrease in REMO, while it shows a slight increase in CLM. Moreover, REMO reveals a wider range of future climate trends than CLM, especially for sunshine, dry days, and heat stress. Both models are driven by the same global coupled atmosphere–ocean model ECHAM5/MPI-OM. Because both models are not able to resolve meso- and micro-scale processes such as cloud microphysics, differences between model results and discrepancies in the development of even those parameters (e.g., cloud formation and cover) are due to different model parameterization and formulation. Climatic changes expected by 2050 are small compared to 2100, but may have major impacts on tourism as for example, snow cover and its duration are highly vulnerable to a warmer climate directly affecting tourism in winter. Beyond indirect impacts are of high relevance as they influence tourism as well. Thus, changes in climate, natural environment, demography, tourists' demands, among other things affect economy in general. The analysis of the CLM results and its comparison with the REMO results complete the analysis performed within the project Climate Trends and Sustainable Development of Tourism in Coastal and Low Mountain Range Regions (CAST) funded by the German Federal Ministry of Education and Research (BMBF).

1 Introduction

Scientific studies about climate change are ongoing and, in some specific areas such as impact assessment they are still at a relatively early stage. Most studies focus on an analysis of climate change in the long term, which currently covers the period up to the end of the present century and includes air temperature and precipitation as the variables most widely used. For impact assessment studies, especially for tourism and recreation, these two variables are not sufficient. By the way, the tourism sector is less interested in what might happen in the end of the twenty-first century. However, the planning horizon in tourism is rather shorter due to its very high flexibility and adaptability.

The reliability of climate models has increased considerably in the past years. The confidence that climate models can provide realistic estimates of future climate is based on their ability to reproduce correctly the present climate due to an improvement of models in various ways, i.e., improved modeling of systems dynamics, higher horizontal and vertical resolutions, more detailed physical parameterization, and

C. Endler (✉) · A. Matzarakis
Meteorological Institute,
Albert-Ludwigs-University of Freiburg,
Werthmannstr. 10,
79085 Freiburg, Germany
e-mail: christina.endler@meteo.uni-freiburg.de

inclusion of more processes (aerosols, land surface, and sea ice) (e.g., Rial et al. 2004, Reichler and Kim 2008).

Although climate change occurs on a global scale, its impacts vary substantially on local and regional scales. Typically, global climate models with a coarse grid resolution (mostly about 100 km) are used to study the effects of increasing greenhouse gas (GHG) concentration, changing aerosol composition and load, as well as land cover changes. These global climate models are not appropriate to represent surface heterogeneities on scales less than about 100 km and to estimate the impact of global change on a regional scale. Therefore, the information obtained by global scale models has to be transferred to smaller scales. A frequently used method to obtain a higher degree of detail in climate projections is achieved by dynamical downscaling using regional (i.e., limited area) climate models (RCM). They are nested into coarser global circulation models (GCM), i.e., they use GCM outputs for calculating a potential climate evolution for the region under consideration. These RCMs are driven by GCM or by meteorological fields from global reanalysis at the boundary of the model domain.

Estimating future climate changes on a regional scale poses certain difficulties as the corresponding terrain (topography, distance to the sea, local wind patterns and their fluctuations, heat island effect of large cities, etc.) has a high impact. Nowadays, climate models can only approximately capture meso- and micro-scale processes during severe weather events. Scenarios for the developments of frequency and intensity of extreme events are, hence, still uncertain. Statistical statements about current trends for extreme events are also difficult because of their rare occurrence (Walkenhorst and Stock 2009).

From 2001 onward, the PRUDENCE project tended to address and reduce the deficiencies in climate projections providing a series of simulations with a grid width of ~50 km and focus on Europe, and to quantify the uncertainties in predictions of future climate using different climate models (PRUDENCE 2007). The ENSEMBLES project (van der Linden and Mitschell 2009), which was funded by the European Commission, run from 2004 to 2009. The project's principal objective was to allow the uncertainty in climate projections to be measured so that a clearer picture of future climate can be formed using very high-resolution regional climate model ensembles (~25 km) for Europe. The exploitation of the results by linking the outputs of the ensemble prediction system to a range of applications ought to be increased. We evaluate – in a smaller context – the performance of regional climate simulations for different forcing scenarios using two RCMs with a grid width below 20 km, as climate change predictions with a grid width of ~50 km or 25 km are still too coarse to be applied to the Black Forest region with its

complex topography. Recently, model results for Europe have become available with grid resolution below 20 km: the CLM consortial simulations using the regional climate model CLM (Steppeler et al. 2003, Böhm et al. 2006, Rockel et al. 2008) and the so-called REMO-UBA simulations (Jacob et al. 2008), generated on behalf of the Federal Environment Agency of Germany by the Max-Planck Institute (MPI) for Meteorology, Hamburg, using the REMO regional climate model (Jacob and Podzun 1997, Jacob 2001, Jacob et al. 2001). The objective of this study is the comparison of results obtained in former studies using the REMO model (Endler and Matzarakis 2010a, b) with results obtained with the CLM model for a complex terrain in the southwest of Germany (Black Forest region). In this context, the analysis is less based on the meteorological parameters air temperature and precipitation, but rather on the thermal component.

The paper is divided into four parts. The first part considers the data based on regional climate modeling and methods deduced from human-biometeorology and tourism climatology. The second part outlines the results derived from the data; afterwards, they will be discussed in part three. The final part summarizes the analysis conducted and will give a further outlook for future investigations.

2 Description of models and methods

Within this study, results of the high-resolution climate simulations performed by the regional climate models REMO and CLM have been analyzed. General characteristics are listed in Table 1. Both models are atmospheric climate models qualified for dynamical nested long-term simulations. Of course, single weather events and their observed occurrence in time and space cannot be expected from climate simulations. Both models are initialized and forced by the global coupled atmospheric–ocean model ECHAM5/MPI-OM (Roeckner et al. 2003, Hagemann et al. 2006, Marsland et al. 2003). The ECHAM5 simulation for the present-day climate uses observed anthropogenic forcing for CO_2, CH_4, N_2O, CFCs, O_3, and sulfate initialized by a pre-industrial control simulation, but neglects natural forcing from volcanoes and changes of solar activity. The future-climate simulations use anthropogenic forcing as described by the respective IPCC SRES emission scenarios. The grid resolution is T63 (1.87 °) with 31 layers.

The REMO model is a hydrostatic climate model which can be used not only in a climate, but also in a forecast mode. In this study, REMO in a climate mode is used (Jacob 2001, Jacob et al. 2001). Processes that cannot be resolved by the model such as convection or turbulences

Table 1 Scheme of the model setups of REMO and CLM

|	REMO	CLM
Model development	MPI for Meteorology, Hamburg	CLM-Community
References	Jacob et al. (2008)	Rockel et al. (2008)
Driving GCM	ECHAM5/MPI-OM	ECHAM5/MPI-OM
Experiment	REMO-UBA simulations	Consortial runs
Horizontal grid resolution	0.088° (10 km×10 km)	0.165° (18 km×18 km)
Vertical grid	27 layers	32 layers
Based on	EM/DM (Europa-Modell and Deutschland-Modell; concerning the dynamical part) ECHAM4 (concerning physical parameterization)	Lokal-Modell (LM)
Model characteristics	Dynamical, hydrostatic,	Dynamical, non-hydrostatic,
	Two-step nesting	Directly nested into GCM
Model domain	Germany, the Alps	Europe
Time period	1950–2100	1960–2100
Emission scenarios	A1B, B1, (A2 is available but not used in this study)	A1B, B1

are estimated by physical parameterization taken from the ECHAM4 climate model (Roeckner et al. 1996). For the REMO-UBA simulations, a two-step nesting was applied. A REMO simulation with a grid width of 0.44° is driven by ECHAM5. This coarser REMO simulation provides the boundary values for the high-resolution REMO-UBA simulation. These climate model runs have a grid width of 0.088° (10 km×10 km) and are available for the three IPCC emission scenarios A1B, B1, and A2 running from 1950 to 2100. The region covered by REMO encompasses Germany and the Alps (Fig. 1, upper panel, left).

In 2001, the local model (LM) of the German Weather Service (DWD) was chosen as basis for a new regional climate model called CLM (climate version of the local model, basis LM 2.19). As many communities are involved in developing the CLM model, the model was renamed as COSMO-CLM, climate limited-area modelling community (CCLM) in 2008 to live up to its name. The CCLM is derived from a routine weather prediction model (Lokalmodell) adapted for climate applications. The CCLM provides high-resolution data with grid widths from 50 to 1 km, and is a non-hydrostatic climate model directly nested into the ECHAM5 field, i.e., it is steadily forced by results of global climate simulations. In this study, simulations with a mesh grid width of 0.165° (18 km×18 km) are used. They are available for Europe (Fig. 1, upper panel, right) for both emission scenarios A1B and B1 running transiently from 1960–2100 (Steppeler et al. 2003, Böhm et al. 2006, Rockel et al. 2008). A brief overview is given in Table 1. Thereinafter, in this study the notation CLM is used. The emission scenarios are accompanied by storylines of social, economic, and technological development. A1B describes a future world of very rapid economic growth and rapid

introduction of new and more efficient technologies. B1 describes a world with rapid changes in economic structures toward a service and information economy, with reductions in material intensity, and the introduction of clean and resource-efficient technologies. In all scenarios, GHG concentrations increase throughout the twenty-first century. The steady incline of GHG concentrations starts to differentiate more distinctly between scenarios only from the year 2040 onward. In that context, A1B entails much more rapid change than B1 (IPCC 2001).

Several climate stations which are run by the DWD were selected for model validation. The following stations were available: Freiburg, Feldberg, Hinterzarten, Titisee, and Bad Wildbad. The data used cover the time period 1961–2000. The nine grid boxes surrounding the measurement station were used to compare mean values and frequency distribution of parameters described below.

This study focuses on the analysis of parameters mentioned below in the complex terrain, namely the Black Forest located in the southwest of Germany (Fig. 1, lower panel). Related to tourism and recreation, the Black Forest states an interesting study site in summer and winter. To assess the climate for tourism and recreation, a method is used which acknowledges all facets of tourism climate, namely the aesthetic, physical, and thermal facets (de Freitas 1990, 2003). The aesthetic facet includes sunshine/cloudiness, visibility, and day length. The physical facet involves rain, wind, snow, severe weather, air quality, and ultraviolet radiation. The thermal facet is characterized by integrated effects of air temperature, wind, solar radiation, humidity, long wave radiation, and metabolic rate, which can be expressed by thermal indices that take into account the body–environment
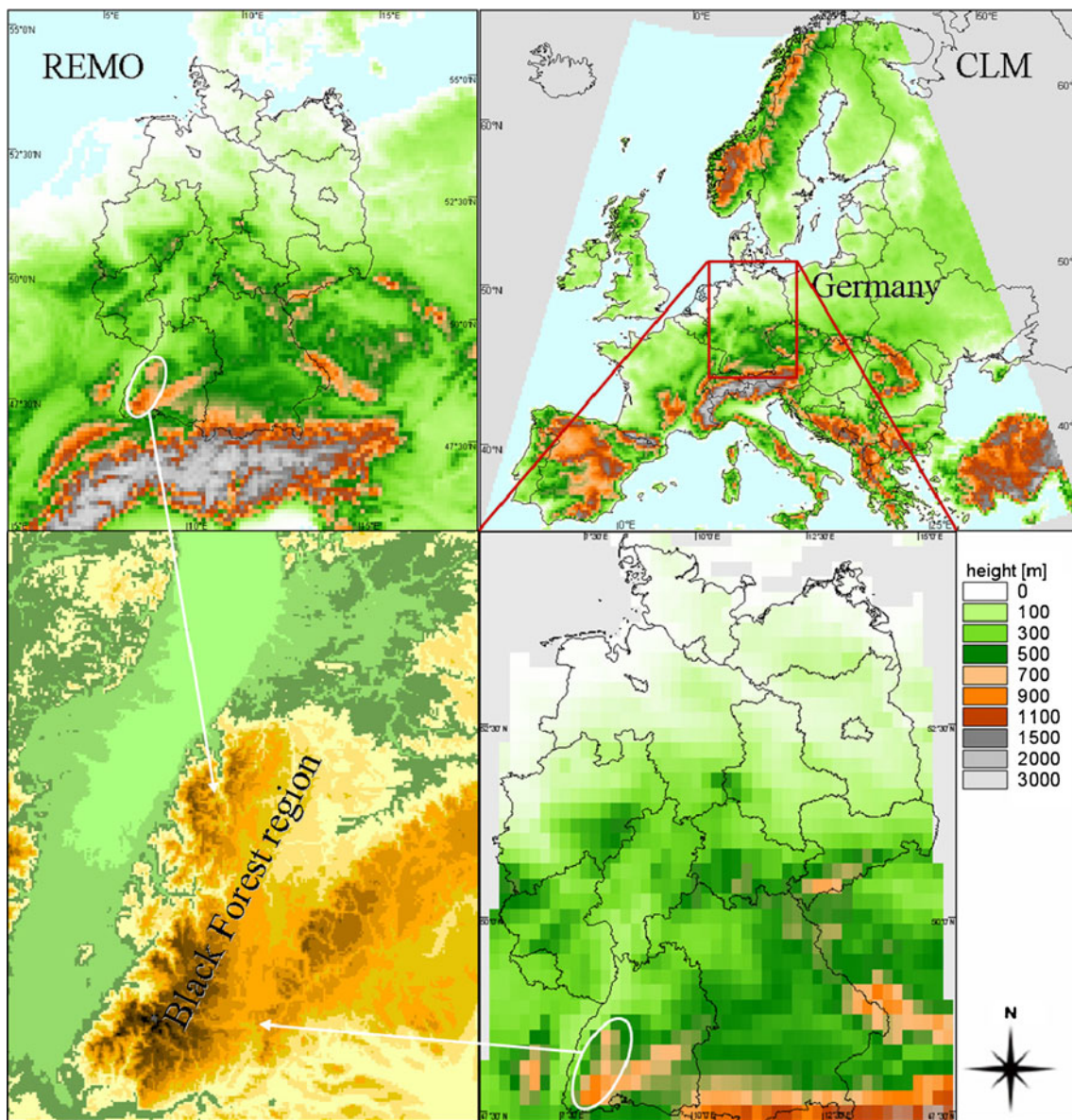
Fig. 1 Model region of REMO (*upper panel, left*) and CLM (*upper and lower panel, right*), as well as the study site of the Black Forest region, southwest of Germany (*lower panel, left*, based on USGS 2004)

energy balance (see Eq. 1) such as the physiologically equivalent temperature (PET, Höppe 1999). All three facets are highly relevant to tourism and recreation (de Freitas 1990, 2003).

$$M + W + Q^*(T_{mrt}, v) + Q_H(T_a, v) + Q_L(e, v)$$
$$+ Q_{SW}(e, v) + Q_{Re}(T_a, e)$$
$$= 0 \qquad (1)$$

In Eq. 1, the energy balance of the human body is given, where M denotes metabolic rate, W energy translation by mechanical power, Q^* radiation balance, Q_H sensible heat flux, Q_L latent heat flux by water vapor diffusion, Q_{SW} latent heat flux by sweat evaporation and Q_{Re} energy translation by respiration. The variables air temperature T_a, wind speed v, vapor pressure e and mean radiant temperature T_{mrt} are relevant for the respective term of the energy balance. In this context, T_{mrt} describes short and long wave radiation fluxes. In this study, PET is calculated using the radiation and energy balance model RayMan (Matzarakis et al. 2007), which includes besides date, longitude, latitude and altitude the following meteorological variables: air temperature, relative humidity or vapor pressure, global radiation or cloud cover, and wind speed reduced at 1.1 m above ground.

A comprehensive approach is utilized to identify the various characteristics of the regional climate. The

following lists the data used over the March to May (MAM), June to August (JJA), September to November (SON), and December to February (DJF) study periods: mean PET, air temperature (Ta) at 2 m above ground, and precipitation (large scale and convective precipitation); number of days with cold stress (PET<0°C); number of days with thermally comfortable condition (18°C<PET<29°C); number of days with heat stress (PET>35°C); number of days with humid-warm conditions (vapor pressure >18 hPa); number of days with cloud cover <4 eighths; number of days with fog, i.e. relative humidity (at 2 m above ground) >93%; number of days with 10 m wind speed >8 ms^{-1}; number of snow days identified as snow water equivalent >5 cm.

The validation between modeled and measured data is based on the comparison of means and partly, frequency distribution. If available, correction factors are applied, for example for air temperature using a generic lapse of +0.65°C per 100 m. Although a correction of air temperature can be applied, this is not the case for global radiation/cloud cover or relative humidity/vapor pressure. As PET accounts for the integrated thermal effect of these variables, a correction factor for PET as a whole is not possible. Because measured snow data are given in snow depth and modeled snow data in snow water equivalent, a conversion is required. In this study, the empirical approach of Brown and Mote (2009) is used, which is based on snow classes introduced by Sturm et al. (1995). If necessary, a correction of 9.91 snow days per 100-m altitude is appropriate according to Witmer (1986).

The model results of the period 2021–2050 are compared to the reference period 1971–2000, i.e., representing only relative changes.

3 Results of CLM and their comparison to REMO

The first step was a validation of the CLM model output with measured data provided by DWD. The model is not able to entirely reproduce the complex topography of the Black Forest region resulting in discrepancies in altitude of the order of up to 600 m. The analysis of the frequency distribution of 2 m Ta modeled by CLM shows a slight overestimation of high values and an underestimation of low values. This is comparable to REMO. However, the differences are lower that means CLM models the climate slightly cooler. The discrepancy seen at 0°C, which is due to modeled melting and freezing processes in the soil, is less pronounced in the CLM compared to the REMO model. Similar results are obtained for PET. In this context, days with heat stress are overestimated, while days with cold stress are underestimated. Precipitation is a highly sensitive meteorological parameter and thus difficult to model, particularly in complex terrains. Although precipitation is quite well reproduced by the model on a large scale, precipitation on a meso- and micro-scale (e.g., convection, orographic lifting, or windward and leeward effects) is less reliable on a mesh grid of 18 or 10 km. Thus, precipitation modeled by REMO is overestimated by almost 20% at lower regions and underestimated by 15–20% at higher regions of the Black Forest, particularly in winter. The other seasons are consistent with measured data. In contrast, CLM overestimates the precipitation both in winter and autumn by 40% and 20%, respectively. Relative humidity is clearly underestimated by REMO, particularly for values from 80% on, and overestimated for values between 50–60%. CLM, however, overesti-

Table 2 Mean annual changes of air temperature, PET, precipitation and the number of days with thermal comfort, cold and heat stress, humid-warm conditions, as well as number of dry, wet, and snow days. Changes in precipitation are specified seasonally. Results (2021/2050 minus 1971/2000) are based on CLM and REMO, and on A1B and B1, respectively. In this context, the range describes changes expected in the Black Forest averaged over the whole region

Parameter	CLM		REMO	
	A1B	B1	A1B	B1
Air temperature	+0.8°C to +1.0°C	+0.5°C to +0.8°C	+0.9°C to +1.1°C	+0.2°C to +0.6°C
PET	+0.8°C to +1.2°C	+0.8°C to +1.0°C	+0.8°C to +1.2°C	−0.2°C to +0.3°C
Thermal comfort	+5 to +10 days	0 to +5 days	−8 to 0 days	−8 to −3 days
Cold stress	−19 to −12 days	−17 to −12 days	−19 to −9 days	−13 to −3 days
Heat stress	+2 to +5 days	0 to +2 days	+2 to +8 days	−3 to +2 days
Humid-warm	12 to +15 days	+6 to +10 days	+8 to +15 days	+4 to +11 days
Precipitation	+10 to +15%	+10%	+5%	+10%
Precipitation (MAM)	15%	−5 to +5%	+35%	+22%
Precipitation (JJA)	±0%	+5 to +10%	−5%	+17%
Precipitation (SON)	+5 to +10%	+10 to +15%	+60%	+33%
Precipitation (DJF)	+25%	+30%	+10%	+30%
Dry days	−10 to −7 days	−12 to −7 days	−5 to +4 days	−14 to −7 days
Wet days	+8 to +12 days	+8 to +10 days	0 to −5 days	+8 to +12 days
Snow days	−12 to −15 days	−9 to −15 days	−12 to −20 days	−8 to −15 days

mates the relative humidity between 90 and 100%. The frequency distribution of vapor pressure shows a clear overestimation of high values in both models. Thus, the number of humid-warm conditions (vapor pressure >18 hPa) tends to be overestimated as well. From this, it follows that thereinafter only relative changes between the base (1971–2000) and future period (2021–2050) are presented based on gridded data.

3.1 Air temperature

An increase in Ta is generally expected to be higher in A1B than in B1 (Table 2), higher in winter up to +1.8°C and in autumn up to +1.6°C than in summer up to +1.2°C and spring up to +0.5°C (REMO). In REMO-B1, the spring is experienced by no changes or even a slight cooling up to −0.7°C. The mean annual increase will be about +0.2°C to +1.1°C. The CLM scenarios show similar results, where autumn will warm up most with an increase of +2.4°C to +2.6°C in A1B that is slightly above average compared to the average temperature increase of Germany of +2.2°C.

Winter warming will be in a range of +0.5°C to +1.5°C and thus below average compared to the average winter temperature of Germany of +1.8°C. Warming in summer and spring is less pronounced with an increase of up to +0.5°C. Seasonal variations thus cause an increase in annual mean of Ta of +0.5°C to +1.1°C. These changes are in a range of ±0.3°C for CLM and ±0.4°C for REMO at the 95% confidence level, hereafter CI95.

3.2 Thermal facet of climate

The thermal facet based on the PET contains both thermal comfort (18°C<PET<29°C, Fig. 2) and discomfort range, namely cold (PET <0°C, Fig. 3) and heat stress (PET >35°C, Fig. 4). A warming throughout the year has more impact on cold stress than on heat stress and thermal comfort (Tables 2 and 3). The most pronounced changes in PET are, according to both models, to be expected during winter and autumn. While REMO models values from +0.9 to +1.8°C in winter and from +0.1°C to +1.6°C in autumn, the results of CLM are in a range between 0.9°C and 1.5°C in winter and
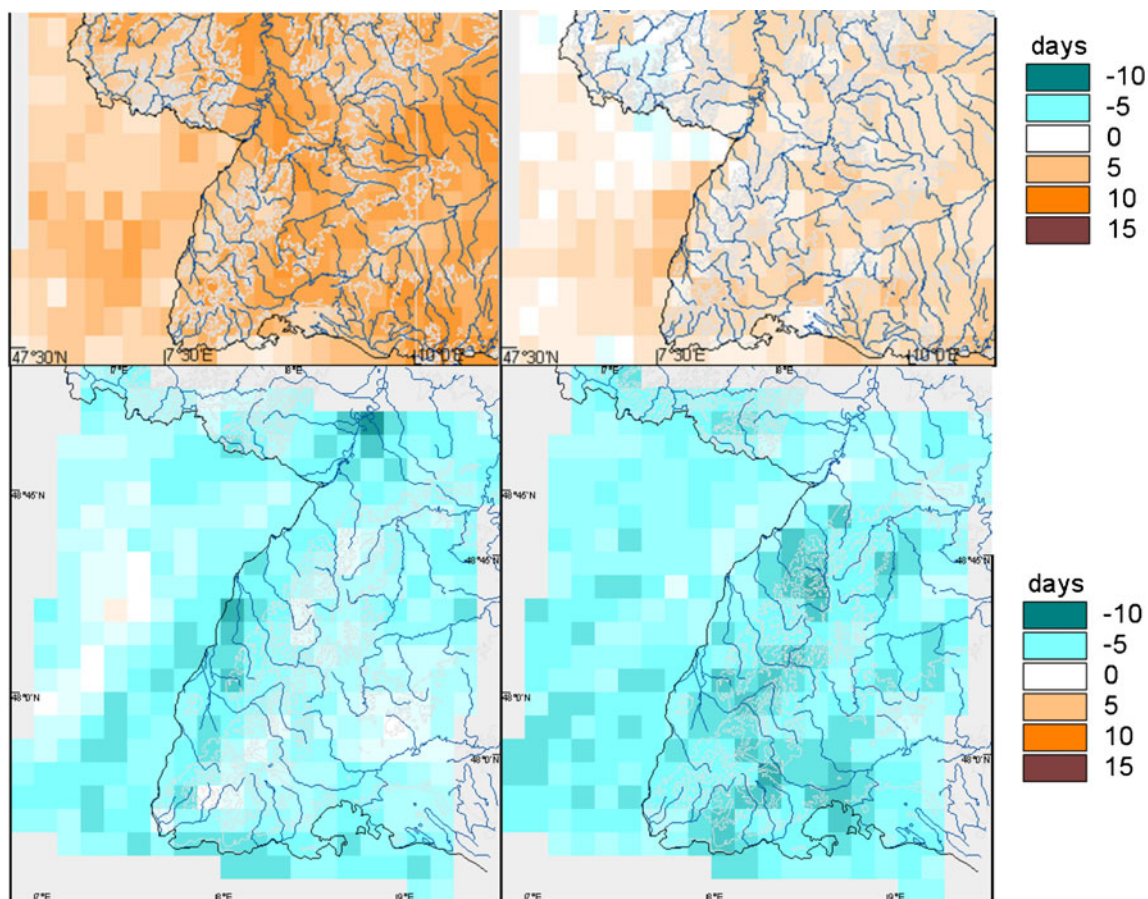
Fig. 2 Changes in the number of days with thermal comfort (18°C<PET<29°C) for 2021–2050 compared to 1971–2000 for CLM-A1B (*upper panel*, *left*) and CLM-B1 (*upper panel*, *right*) and for REMO-A1B (*lower panel*, *left*) and REMO-B1 (*lower panel, right*)
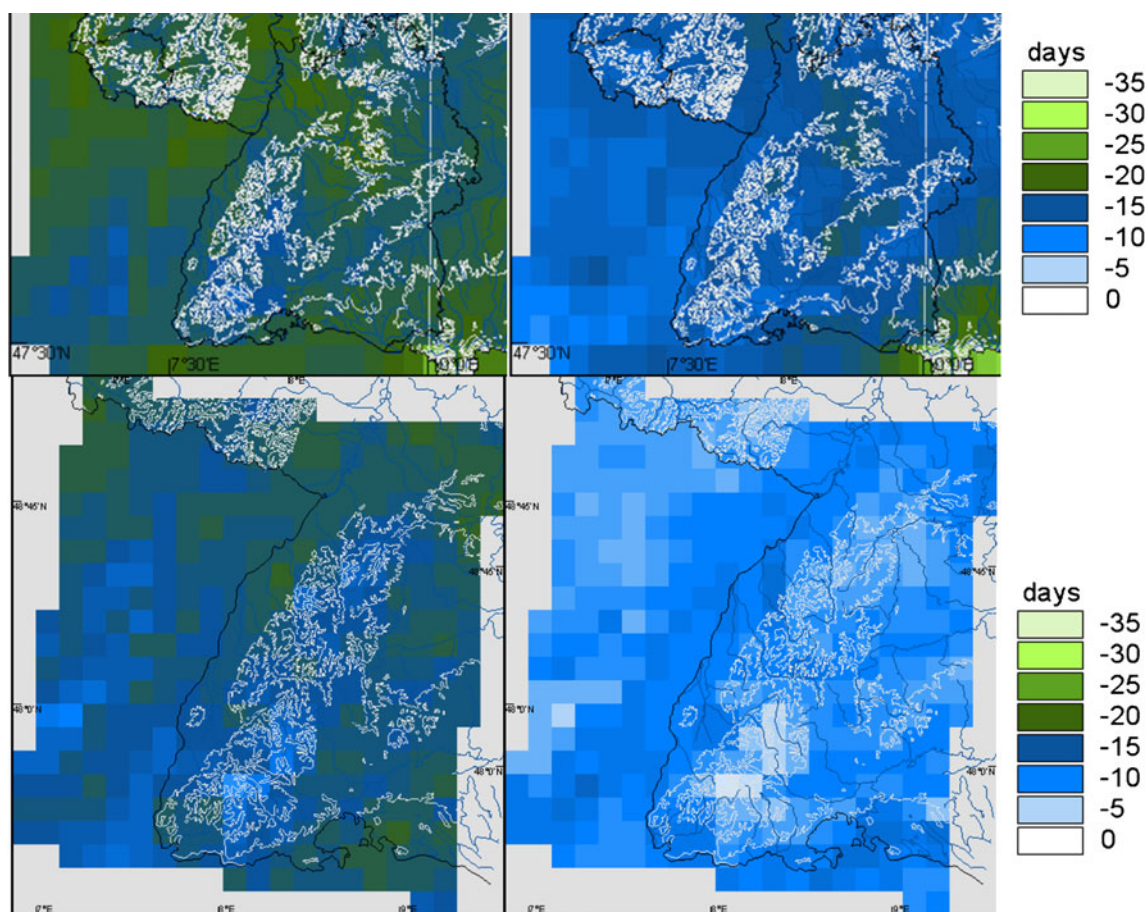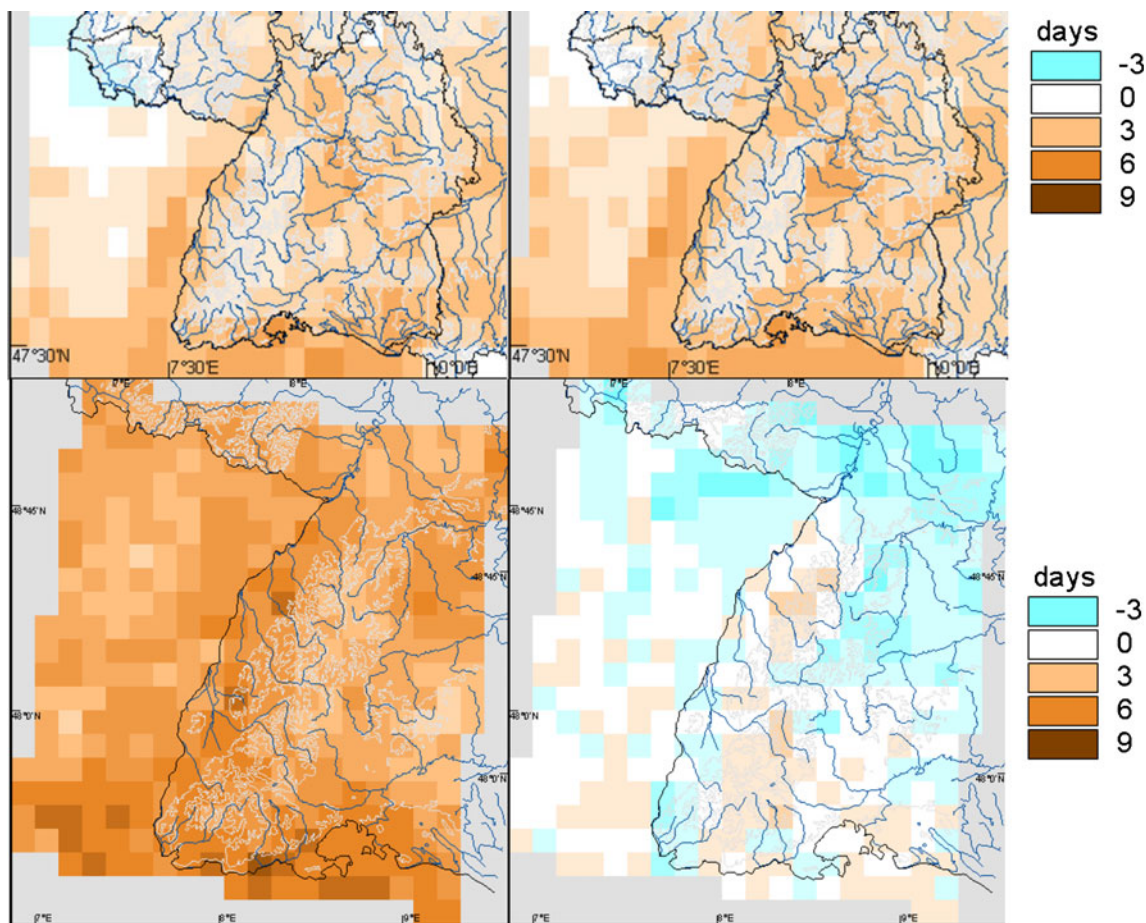
Fig. 3 Changes in the number of days with cold stress (PET <0°C) for 2021–2050 compared to 1971–2000 for CLM-A1B (*upper panel*, *left*) and CLM-B1 (*upper panel*, *right*) and for REMO-A1B (*lower panel, left*) and REMO-B1 (*lower panel, right*)

between 1.8°C and 3.0°C in autumn. The warming results in a stronger decrease in cold stress by about 4 to 15 days in winter – higher altitudes are hardly affected – compared to autumn, where it decreases by about 5 days. A slight increase in the number of days with thermal comfort of about 5 days is expected in autumn, except in REMO-B1. Also here, higher altitudes are hardly affected. Changes in summer PET based on CLM are in a range between +0.5°C and +0.7°C, whereas changes based on REMO are somewhat heterogeneous: an increase by +0.9°C to 1.6°C is expected in A1B, and changes in a range between −0.6°C and +0.1°C in B1. Warming during spring according to CLM is in the same range as summer warming, except for B1. Thus, PET will increase up to +1.5°C, causing a slight decrease in cold stress by 5 days at maximum. According to REMO, springtime is experienced by cooling up to −0.7°C and −1.3°C, respectively, resulting in a slight increase in cold stress. Changes in PET values are in a range of ±0.4°C for CLM and REMO at the CI95. Changes in cold stress are for both models in a range of ±5 days at the CI95. Heat stress will somewhat increase, but only in summer. Higher regions and

the northern part of the Black Forest show no significant changes. Changes in thermally comfortable conditions show a heterogeneous distribution throughout the year. CLM models a mean annual increase by +5 to +10 (CI95: ±5 days) with the main contribution in autumn as mentioned before (only in A1B) and infrequently in summer and spring. In addition, a slight decrease could be expected infrequently in summer. REMO, on the contrary, simulates a mean annual decrease up to −10 (CI: ±5 days), except for higher altitudes that are hardly affected. The main reduction will be noticed primarily in spring and summer, where the latter could also be experienced by a slight increase in B1.

Humid-warm conditions (vapor pressure >18 hPa) can be related to both the thermal and physical facets, and is outlined in this section. By 2050, an increase in the number of humid-warm conditions of about +4 to +15 (CI95: ±3 days) is expected in both models where the increase is somewhat more pronounced in A1B (Fig. 5, Tables 2 and 3). In this context, the summer season will be predominately affected, while spring and autumn show very little changes.

Fig. 4 Changes in the number of days with heat stress (PET>35°C) for 2021-2050 compared to 1971-2000 for CLM-A1B (*upper panel*, *left*) and CLM-B1 (*upper panel*, *right*) and for REMO-A1B (*lower panel, left*) and REMO-B1 (*lower panel, right*)

3.3 Physical facet of climate

The physical facet includes the following parameters: precipitation, snow, and wind. According to both models, changes in mean annual precipitation amount are about +5% to +15 % (Table 2). In this context, changes in winter precipitation by nearly 30% entail the highest changes to the annual mean. Changes based on REMO-A1B are 10% somewhat smaller. Major changes of +33% to +60% modeled by REMO will also be expected in autumn. In CLM, changes in autumn precipitation are in a range between +5% and +15%. While changes in summer precipitation based on CLM will contribute with 0% to +15% to changes in the annual mean, changes based on REMO entail with −5% to +17% to changes in the annual mean. Changes in spring precipitation are modeled by both models in a similar range: an increase by +22% to +35% in REMO and both an increase of +5% and decrease of −5% in CLM (Table 2).

Changes in the number of days with less precipitation (precipitation ≤1 mm) reflect changes similar to the annual precipitation pattern, i.e., dry days tend to decrease about −14 to −5 days (Fig. 6, Tables 2 and 3). However, the pattern will be more heterogeneous on a seasonal scale. Spring and autumn (MAM and SON) tend to be experienced by a marginal decrease in dry days, except for CLM-A1B. While summer is hardly affected by changes in dry days in CLM, they tend to slightly increase in REMO, with the exception of REMO-B1. During winter, dry days are expected to strongly decrease in both models, except for REMO-A1B. Snow days defined as snow water equivalent greater than 5 cm will be reduced up to 20 days (REMO) and 15 days (CLM) by 2050 (Fig. 7, Tables 2 and 3). In this context, changes are in a range of ±6 days at the CI95. Changes in windy days (wind velocity >8 ms^{-1}) are not significant in the two models (Table 3).

3.4 Aesthetic facet of climate

Data output from REMO and CLM for cloud cover and fog (relative humidity >93%) that comprise the aesthetic facet of climate in tourism showed that there were only small changes between present and future climate; but these changes are not significant at the CI95 (Table 3).

In summary, Table 2 quantitatively lists all parameters analyzed in this study for both models and scenarios. Table 3 condenses this information into a purely qualitative summary.

4 Discussion

In order to complete the set of analyses for Black Forest, this study focuses on both the results of the CLM model and their comparison to REMO obtained previously (Endler and Matzarakis 2010a, b, Endler et al. 2010). In general, regional climate models are able to reproduce the climate, but uncertainties are still remaining, although the physics underlying is mostly understood (Rial et al. 2004, Reichler and Kim 2008). Uncertainties, especially in regional climate modeling, are due to the driving global circulation model among others. There is no established way to tell which model represents the most probable version of the future climate, as a comparison of models reveals discrepancies in their results (e.g., showing partly different atmospheric conditions, especially in complex topography). Thus, uncertainty can be evaluated either by performing several simulations with the same model or using different climate models with the same forcing (Déqué et al. 2007). Both approaches can be combined, as for example, in PRUDENCE (2007) and ENSEMBLES (van der Linden and Mitschell 2009).

For a nested model as CLM and REMO, it is well known that the ability to simulate inter-annual variability

Table 3 A qualitative summary of the number of days with thermal comfort, cold and heat stress, humid-warm, sunny, dry, wet, foggy and windy conditions, as well as snow days that are analyzed for the Black Forest region are based on the two regional climate models CLM and REMO

Parameter	CLM	REMO
Thermal comfort	+	−
Cold stress	−−	−−
Heat stress	+	n. s.
Humid-warm conditions ("sultry")	++	++
Sunny	−	*n. s.*
Dry	−	n. s.
Wet	+	+
Foggy	+	+
Windy	*0*	*0*
Snow days	−−	−−

The notation −−/++ defines a moderate decrease/increase, −/+ a slight decrease/increase, *0* no changes in the model, and *n. s.* not specified due to huge variations between the scenarios A1B and B1. Italicized parameters are expected to not change significantly in the entire region at the 95% confidence interval

depends, to a high degree, on the quality of the driving model, and in particular, on the degree to which the driving model represents the observed flow conditions for the region of concern (e.g., Machenhauer et al. 1998, Giorgi et al. 2001). Some authors, e.g., Rowell (2006) and Déqué et al. (2007) stated that the largest uncertainty is introduced by the choice of the driving GCM, rather than the evolution of emission and GHG concentration or RCM formulation. Thus, it would be worthwhile to identify the quality of ECHAM5, the driving GCM.
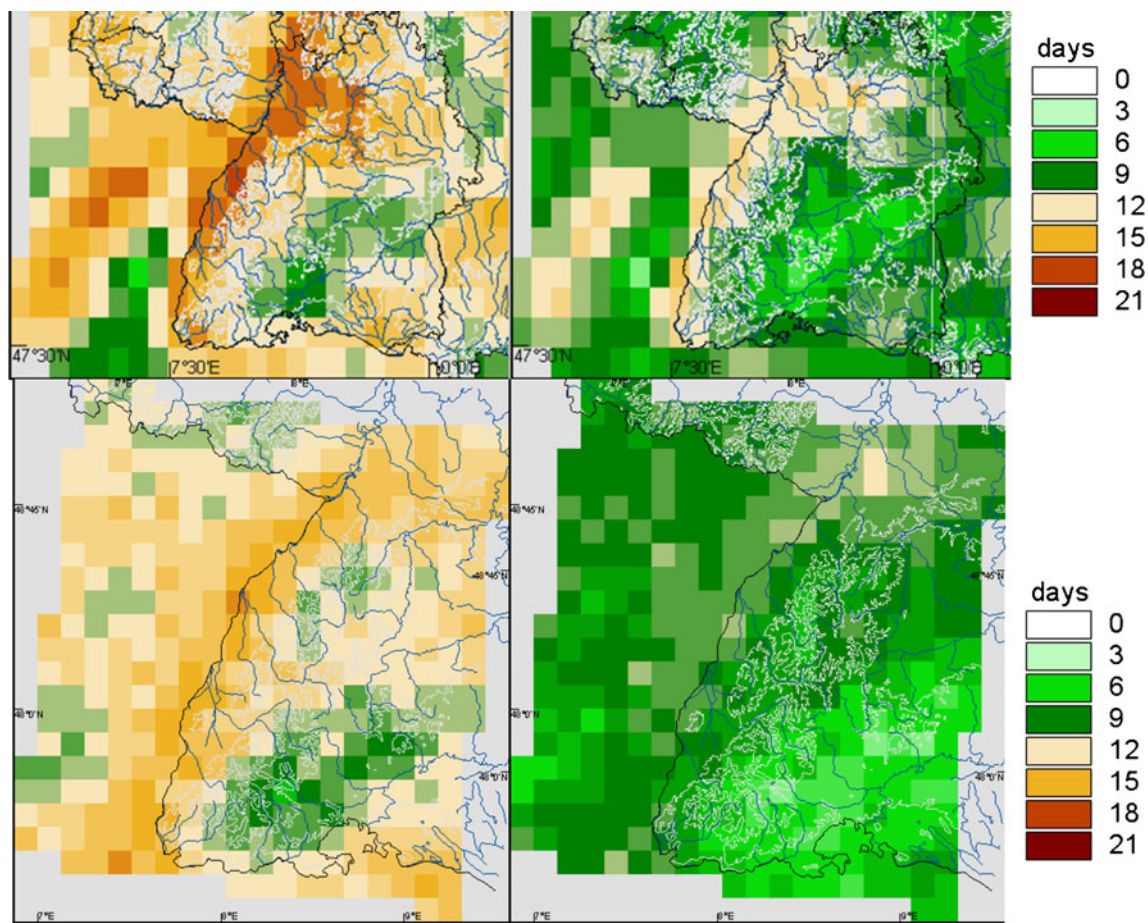
Van Ulden and van Oldenborgh (2006) validated several GCMs with the result that ECHAM5/MPI-OM is one of the most accurate global circulation models although summer circulations in northern latitudes (30°–90°N) are shown to be difficult to simulate correctly (Demuzere et al. 2009). In this context, westerly circulation is significantly overestimated, while easterly circulation is underestimated (Demuzere et al. 2009). Further studies concerning ECHAM5 are available for the validation of the (1) hydrological cycle (e.g., Hagemann et al. 2006), (2) snow component (e.g., Roesch and Roeckner 2008), and (3) temperature distribution and temperature–precipitation-based indices (e.g., Sillmann and Roeckner 2008). Altogether, ECHAM5 realistically simulates the mean climate and its variability with slight underestimations of variability in late winter (van Ulden and van Oldenborgh 2006). Indeed, a good performance of present-day climate does not imply a good performance of climate change projections. Moreover, recent models have a higher quality compared to the previous generation as found by Reichler and Kim (2008) who compared the results from three generations of the Coupled Model Intercomparison Project (PCMDI 2007) models.

The results here presented reveal that both models tend to simulate the same mean annual tendencies, except for thermal comfort based on PET. PET is calculated from four main meteorological input variables such as air temperature, vapor pressure or air humidity, global radiation or cloud cover, and wind speed reduced at 1.1 m that describes the gravity center of humans. Therefore, uncertainties can arise as, for instance, wind and cloud are difficult to model (cf. Kropp and Scholze 2009), especially in complex terrain such as the Black Forest. While PET in spring is experienced to decrease in REMO, PET in autumn will have stronger increase in CLM. The impact of seasonal results can exceed the influence of the annual mean. This results in a corresponding trend of decrease in REMO and increase in CLM, respectively. Hence, a closer look at the seasonal scale and the detection of its single impact would be worthwhile. Additionally, a general warming causes a shifting to higher PET values and hence, a modification of its frequency distribution. Because these changes are more experienced in colder seasons than in warmer seasons,

Fig. 5 Changes in the number of days with humid-warm conditions (vapor pressure >18 hPa) for 2021–2050 compared to 1971–2000 for CLM-A1B (*upper panel, left*) and CLM-B1 (*upper panel, right*) and for REMO-A1B (*lower panel, left*) and REMO-B1 (*lower panel, right*)

spring (MAM) and autumn (SON), as well as the winter season, might be more affected by changes in the thermal environment.

The largest differences between the two models occur in the off- and summer season. The dependency of RCM on GCM is, due to a stronger atmospheric circulation in that period, strongest in winter. The RCM formulation and parameterization implemented thus contribute distinctively to the resulting uncertainties. This could explain the discrepancies between the two models, in particular for variables affected by parameterization is consistent – in the broader sense – with the findings of Wang (2005) who confirmed that the response of an individual model may differ from a multi-model response because it includes improved parameterization, or because it includes a mechanism or feedback that the other models do not have.

Distinguishable differences between the two scenarios are hardly seen before 2040 due to a rather homogenous evolution of emission and GHG concentration in the beginning of the simulation period. Schröter et al. (2005) conclude that differences between models are often larger

than between different emission scenarios. Although different climate scenarios of REMO and CLM coincide in many basic tendencies, the climate change projections partly produce contradicting trends, particularly in REMO. REMO simulations show higher differences between A1B and B1 than CLM; for instance, for heat stress and precipitation–cloud cover indices (cf. Table 3). These discrepancies are to be ascribed to RCM formulation and parameterization because CLM does not show any contradicting trends in the thermal environment and is driven by the same GCM. Contradicting trends in heat stress can be explained by the different development in summer PET in the two scenarios considered. Apart from that, cloud cover and precipitation are difficult to model. Why REMO is more sensitive to little differences in emissions scenarios remains unsolved.

It is known that precipitation and snow are very variable and difficult to model, especially in complex terrain. While the general character of the mountain influence has been captured, differences in snow class from valleys to the mountain tops are not shown at that resolution. The reproduction of the spatial distribution of precipitation also
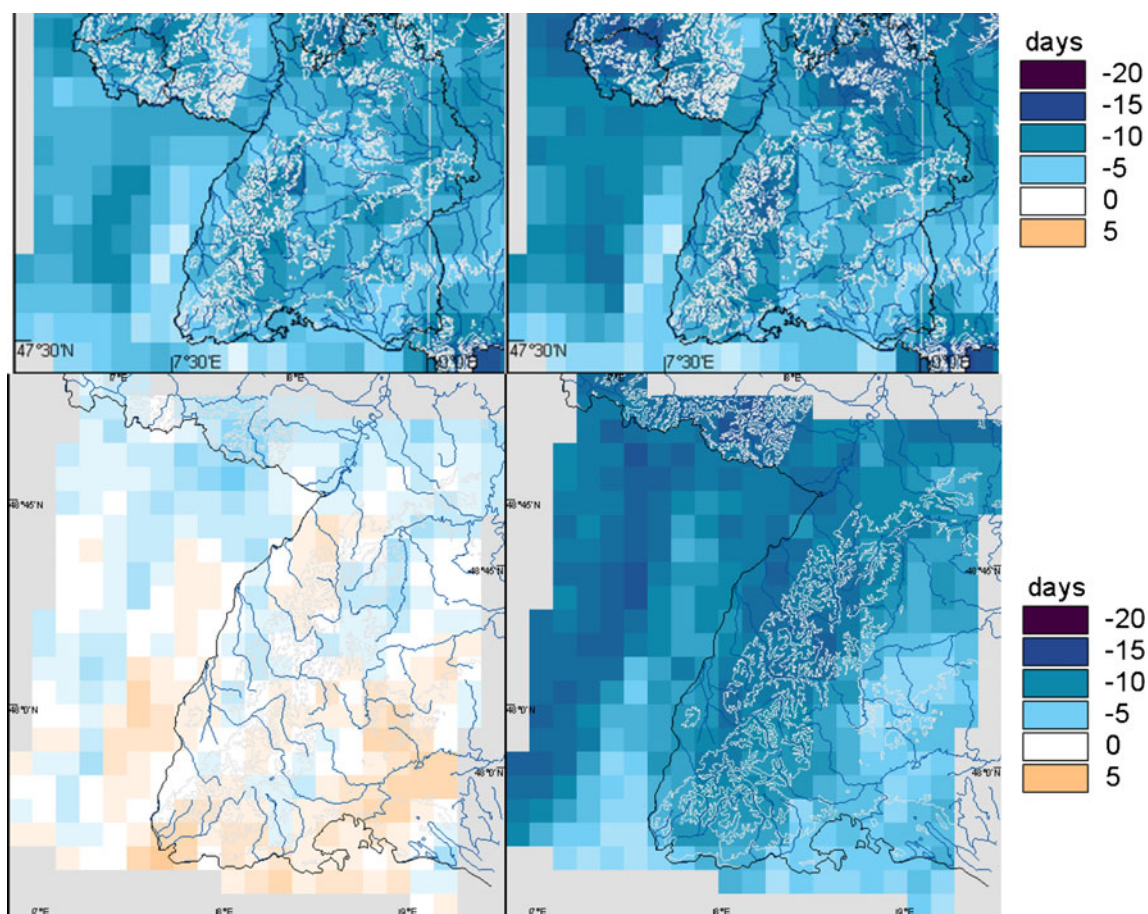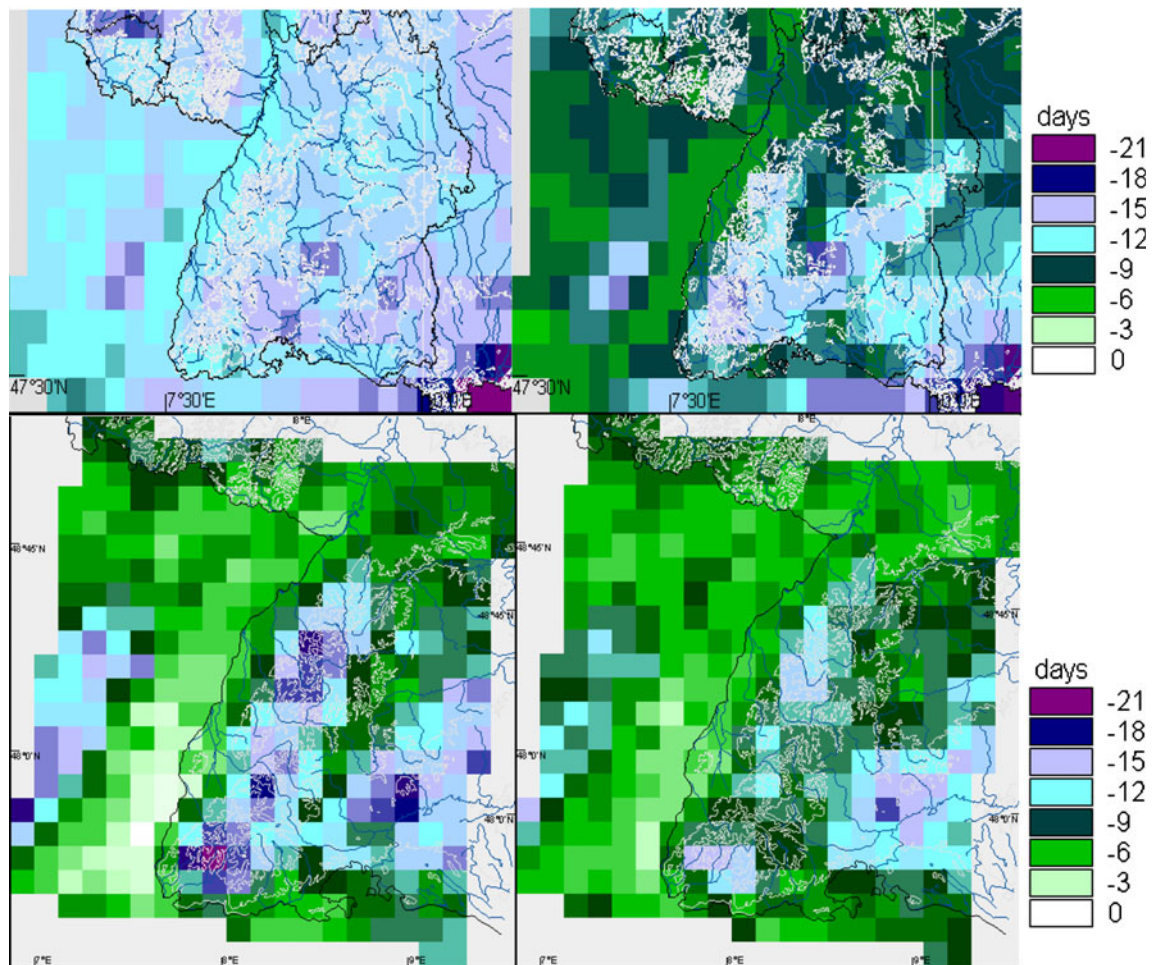
Fig. 6 Changes in the number of dry days (precipitation ≤1 mm) for 2021–2050 compared to 1971–2000 for CLM-A1B (*upper panel*, *left*) and CLM-B1 (*upper panel*, *right*) and for REMO-A1B (*lower panel, left*) and REMO-B1 (*lower panel, right*)

poses a great challenge for the RCMs of the last generation (Sturm et al. 1995).

Feldmann et al. (2008) stated that regional climate models such as REMO and CLM are indeed able to reproduce realistically the precipitation pattern, e.g., in southwestern Germany, but its total is overestimated in lower and underestimated in higher region by REMO (Endler and Matzarakis 2010a, b), whereas CLM models the climate too wet, particularly in winter (cf. Jacob et al. 2007, Feldmann et al. 2008). These results can be partly explained by the known tendency of ECHAM5 overestimating the winter precipitation over Europe (Hagemann et al. 2006). In summer, when smaller scale processes are more important, and in spring as well as autumn, when the general circulation is changing to a more convective or stratus circulation (affected again more by the driving GCM) CLM and REMO results vary. The advantage of regional models with a higher spatial resolution and therefore, a more detailed treatment of physical processes becomes apparent in producing precipitation fields closer to the observations (Han and Roads 2004). By the way, the way of implementing physical processes such as cloud microphysics, and whether models include prognostic cloud water and precipitation is important. In this context, REMO does not include prognostic precipitation, CLM does, but it was not switched on in the consortial simulations. Differences in precipitation have arisen by the model might be explained by parameterization of microphysical processes.

Although Walkenhorst and Stock (2009) point to use at least two or more emission scenarios, global and regional climate models, our results show that two RCMs are not sufficient in order to obtain reliable information for a complex terrain. Thus, it would be worthwhile to make the same analysis by driving different models with the same boundary conditions as recommended by e.g., Crossley et al. (2000) or to use a multi-model approach (e.g., Branković et al. 2010) like ENSEMBLES. Rind (2008) however, doubts that uncertainties in climate model responses which are largely due to different model physics will be reduced by a multi-model approach. "Averaging different model formulations" may not improve results and Wang (2005) pointed out that the consistency among climate models does not necessarily imply improved reliability.

Fig. 7 Changes in the number of snow days (SWE >5 cm) for 2021–2050 compared to 1971–2000 for CLM-A1B (*upper panel*, *left*) and CLM-B1 (*upper panel*, *right*) and for REMO-A1B (*lower panel, left*) and REMO-B1 (*lower panel, right*)

Changes expected by 2050 are relatively small compared to 2100. But their impacts can partly be serious from a point of view of tourism climatology. An increase in air temperature, for example, has a vast impact on winter sport conditions that means a decrease in snow cover and its duration. This reduction of the winter sport season implies a threat for tourism in winter and tourism industry, in general (Endler and Matzarakis 2010a). For example, an increase in air temperature of 1°C raises the snow line about 150 m (Beniston 2003). As tourism in winter is of high relevance in the Black Forest, little changes in climate have a major indirect impact. An increase in heat stress and humid-warm conditions, particularly during the warmer seasons, affects humans' health and activities. In this context, both summer season and lower altitudes are predominately affected. Climate change will not only impact on tourism directly, but also indirectly, as it will transform the natural environment such as changing biodiversity or scenery among other things that attracts tourists in the first place and the image of the destination, which is also a decisive factor (Endler and Matzarakis 2010b).

5 Conclusion

The presented analysis completes the evaluation and quantification of climate change for tourism and recreation within the CAST project using two regional climate models, REMO and CLM, and two scenarios, A1B and B1. The comparison provides insight into the differences between regional climate simulations and which characteristics of agreement with observations are common despite differences in model formulation. In this context, it could be shown that a closer look at a seasonal scale is worthwhile, since several annual trends are strongly caused and determined by single seasons. For tourism and recreation, especially in the context of adaptation measures, a seasonal analysis is required.

Model results coincide in many basic tendencies for the time span 2021–2050 compared to 1971–2000: an increase in humid-warm, wet conditions and a decrease in cold stress, snow depth and snow days. The degree of changes varies with the model. But differences are dependent on both model and scenario. In comparison to CLM, REMO

shows quite often scenario-dependent differences, especially for heat stress, dry and sunny days, although the evolution of emission and GHG concentration is quite homogenous until 2040. Only changes in thermal comfort calculated from four meteorological parameters, each afflicted by individual modeling uncertainties, are contradicting. While CLM models an increase in, REMO models a decrease of thermal comfort that varies considerably on a seasonal scale.

In general, climate impact research provides relevant information; therefore, the challenge for e.g., stakeholders is to manage the uncertainty, because estimates of future climate from RCM simulations are affected by several types of uncertainties including, e.g., specification of emission scenario, changes in land use, boundary conditions from global climate models, and RCM model formulation. Some parameters are more robust such as air temperature, some are less such as precipitation, snow, wind, or cloud cover. Thus, two models are not sufficient in order to obtain reliable information for the Black Forest region. As both models are driven by the same global model, and it is assumed that the largest uncertainty is introduced by the driving model, most of the modeling differences can be ascribed to parameterization.

From a point of view of tourism climatology, little climate changes expected by 2050 may have major impacts on the vulnerability of tourism, as indirect impacts such as change in demography and tourists' demands affect tourism as well. In order to be competitive, tourism tends to all-year tourism. Therefore, it is required to quantify climatically direct and indirect changes in order to estimate the trend of tourism and to maintain the tourism industry.

References

Beniston M (2003) Climatic change in mountain regions: a review of possible impacts. Clim Change 59:5–31

Böhm U, Kücken M, AhrensW BA, Hauffe D, Keuler K, Rockel B, Will A (2006) CLM – the climate version of LM: brief description and long-term application. COSMO Newsletter 6:225–235

Branković C, Srnec L, Pataračić M (2010) An assessment of global and regional climate change based on the EH5OM climate model ensembles. Clim Change 98:21–49

Brown RD, Mote PW (2009) The response of northern hemisphere snow cover to a changing climate. J Clim 22:2124–2145

Crossley JF, Polcher J, Cox PM, Gedney N, Planton S (2000) Uncertainties linked to land-surface processes in climate change simulations. Clim Dyn 16:949–961

De Freitas CR (1990) Recreation climate assessment. Int J Climatol 10:89–103

De Freitas CR (2003) Tourism climatology: evaluating environmental information for decision making and business planning in the recreation and tourism sector. Int J Biometeorol 48:45–54

Demuzere M, Werner M, van Lipzig NPM, Roeckner E (2009) An analysis of present and future ECHAM5 pressure fields using a classification of circulation patterns. Int J Climatol 29:1796–1810

Déqué M, Rowell DP, Lüthi D, Giorgi F, Christensen JH, Rockel B, Jacob D, Kjellström E, de Castro M, van den Hurk B (2007) An intercomparison of regional climate simulations for Europe: assessing uncertainties in model projections. Clim Change 81:53–70

Endler C, Matzarakis A (2010a) Climatic potential for tourism in the Black Forest, Germany – winter season. Int J Biometeorol. doi:10.1007/s00484-010-0342-0

Endler C, Matzarakis A (2010b) Climate and tourism in the Black Forest during the warm season. Int J Biometeorol. doi:10.1007/s00484-010-0323-3

Endler C, Oehler K, Matzarakis A (2010) Vertical gradient of climate change and climate tourism conditions in the Black Forest. Int J Biometeorol 54:45–61

Feldmann H, Früh B, Schädler G, Panitz H-J, Keuler K, Jacob D, Lorenz P (2008) Evaluation of the precipitation for Southwestern Germany from high resolution simulations with regional climate models. Met Z 17(4):455–465

Giorgi F, Hewitson B, Christensen JH, Hulme M, von Storch H, Whetton P, Jones R, Mearns L, Fu C (2001) Regional climate information—evaluation and projections. In: Houghton J et al (eds) Climate change 2001: the scientific basis. Intergovernmental Panel on Climate Change. Cambridge University Press, Cambridge, Cambridge

Hagemann S, Arpe K, Roeckner E (2006) Evaluation of the hydrological cycle in the ECHAM5 model. J Climate 19:3810–3827

Han J, Roads JO (2004) U.S. climate sensitivity simulated with NCEP regional spectral model. Clim Change 62:115–154

Höppe P (1999) The physiological equivalent temperature – a universal index for the biometeorological assessment of the thermal environment. Int J Biometeorol 43:71–75

IPCC (2001) Climate change 2001: the scientific basis. In: Houghton JT et al (eds) Contribution of the Working Group I to the third assessment report of the Intergovernmental Panel on Climate Change. Cambridge University Press, Cambridge

Jacob D (2001) A note on the simulation of the annual and inter-annual variability of the water budget over the Baltic Sea drainage basin. Meteorol Atmos Phys 77:61–73

Jacob D, Podzun R (1997) Sensitivity studies with the regional climate model REMO. Meteorol Atmos Phys 63:119–129

Jacob D, van der Hurk BJJM, Andræ U, Elgered G, Graham L-P, Fortelius C, Jackson SD, Kartens U, Chr K, Lindau R, Podzun R, Roeckel B, Rubel F, Sass BH, Smith RNB, Yang X (2001) A comprehensive model inter-comparison study investigating the water budget during the BALTEX PIDCAP period. Meteorol Atmos Phys 77:19–43

Jacob D, Bärring L, Christensen OB, Christensen JH, de Castro M, Déqué M, Giorgi F, Hagemann S, Hirschi M, Jones R, Kjellström E, Lenderink G, Rockel B, Sánchez E, Schär C, Seneviratne SI, Somot S, van Ulden A, van den Hurk B (2007) An inter-comparison of regional climate models for Europe: model performance in present-day climate. Clim Change 81:31–52

Jacob D, Göttel H, Kotlarski S, Lorenz P, Sieck K (2008) Klimaauswirkungen und Anpassung in Deutschland. Phase 1: Erstellung regionaler Klimaszenarien für Deutschland. Climate Change 11/2008, UBA-FBNr: 000969 Förderkennzeichen: 20441138, Umweltbundesamt. Dessau-Roßlau

Kropp J, Scholze M (2009) Climate change information for effective adaptation – a practitioner's manual. Deutsche Gesellschaft für Technische Zusammenarbeit GmbH(GTZ) Climate Protection Programme, Eschborn

Machenhauer B, Windelband M, Botzet M, Christensen JH, Déqué M, Jones RG, Ruti PM, Visconti G (1998) Validation and analysis of regional present-day climate and climate change simulations over Europe. Max Planck Institut für Meteorologie Report 275, MPI, Hamburg, Germany

Marsland GA, Haak H, Jungclaus JH, Latif M, Röske F (2003) The Max Planck Institute global/sea-ice model with orthogonal curvilinear coordinates. Ocean Model 5:91–127

Matzarakis A, Rutz F, Mayer H (2007) Modelling radiation fluxes in simple and complex environment—application of the RayMan model. Int J Biometeorol 51:323–334

PCMDI (2007) IPCC model output. Available online at www-pcmdi.llnl.gov/ipcc/about_ipcc.php

PRUDENCE (2007) Prediction of regional Scenarios and Uncertainties for Defining European Climate Change Risks and Effects: The PRUDENCE Project. Climatic Change 81 Supplement 1:1-371

Reichler T, Kim J (2008) How well do coupled models simulate today's climate? Bull Am Meteorol Soc 89:304–311

Rial JA, Pielke RA, Beniston M, Claussen M, Canadell J, Cox P, Held H, de Noblet-Ducoudré N, Prinn R, Reynolds JF, Salas JD (2004) Nonlinearities, feedbacks and critical thresholds within the earth's climate system. Clim Change 65:11–38

Rind D (2008) The consequences of not knowing low- and high-latitude climate sensitivity. Bull Am Meteorol Soc 89:855–864

Rockel B, Will A, Hense A (2008) The regional climate model COSMO-CLM (CCLM), Editorial. Met Z 12(4):347–348

Roeckner E, Arpe K, Bengtsson L, Christoph M, Claussen M, Dümenil L, Esch M, Giorgetta M, Schlese U, Schulzweida U (1996) The atmospheric general circulation model ECHAM4: model description and simulation of present-day climate. Max Planck Institute for Meteorology, Report No. 218. Hamburg

Roeckner E, Bäuml G, Bonaventura L, Brokopf R, Esch M, Giorgetta M, Hagemann S, Kirchner I, Kornblueh L, Manzini E, Rhodin A, Schlese U, Schultzweida U, Tompkins A (2003) The atmospheric general circulation model ECHAM5. Part I: model description. Max Planck Institute for Meteorology, Report No. 349. Hamburg

Roesch A, Roeckner E (2008) Assessment of snow cover and surface albedo in the ECHAM5 general circulation model. J Climate 19:3828–3843

Rowell DP (2006) A demonstration of the uncertainty in projection of the UK climate change resulting from regional climate model formulation. Clim Change 79:243–257

Schröter D, Zebisch M, Grothmann T (2005) Climate change in Germany – vulnerability and adaptation of climate-sensitive sectors. Klimastatusbericht DWD 2005:44–56

Sillmann J, Roeckner E (2008) Indices for extreme events in projections of anthropogenic climate change. Clim Change 86:83–104

Steppeler J, Doms G, Schaettler U, Bitzer HW, Gassmann A, Damrath U, Gregoric G (2003) Meso-gamma scale forecasts using the nonhydrostatic model LM. Meteorol Atmos Phys 82:75–96

Sturm M, Holmgren J, Liston GE (1995) A seasonal snow cover classification system for local to global applications. J Climate 8:1261–1283

USGS (2004) Shuttle radar topography mission, 30 arc second scene SRTM_GTOPO_u30_n090e020, unfilled unfinished 2.0, Global Land Cover Facility, University of Maryland, College Park, Maryland, July 2004

Van der Linden P, Mitchell JFB (2009) ENSEMBLES: climate change and its impacts: summary of research and results from the ENSEMBLES projection. Final report. Met Office Hadley Centre, Exeter

Van Ulden AP, van Oldenborgh GJ (2006) Large-scale atmospheric circulation biases and changes in global climate model simulations and their importance for climate change in Central Europe. Atmos Chem Phys 6:863–881

Walkenhorst O, Stock M (2009) Regionale Klimaszenarien für Deutschland. Eine Leseanleitung. E-Paper der ARL, Nr. 6. Akademie für Raumforschung und Landesplanung, Hannover

Wang G (2005) Agricultural drought in a future climate: results from 15 global climate models participating in the IPCC 4th assessment. Clim Dyn 25:739–753

Witmer U (1986) Erfassung, Bearbeitung und Kartierung von Schneedaten in der Schweiz. Geographica Bernesia G25